



DE05FA181



DE021407426

The Theta-Pinch -- A Versatile Tool for the Generation and Study of High Temperature Plasmas

E. Hintz

*Institut fuer Plasmaphysik, Forschungszentrum-Juelich GmbH, Germany
E.Hintz@fz-juelich.de*

ABSTRACT

The more general technical and physical features of theta-pinches are described. Special field of their application are high- β plasmas. Two examples are analysed and studied in more detail: a high density plasma near thermal equilibrium and a low density plasma far from equilibrium. The latter is of special interest for future investigations. Possibilities of field-reversed configurations are pointed out.

Key words: Hydrogen Plasma, Fast Magnetic Compression, Current Sheath, Collisionless Dissipation

INTRODUCTION

The main intention of this contribution is to recall the good suitability of the theta-pinch technique for the study of high temperature plasmas, in particular, of high- β plasmas. After some introductory remarks on the more general characteristics of theta-pinches^{(1),(2)}, we present two experimental situations in more detail. The first one, where a hydrogen plasma with temperatures of a few hundred eV and conditions close to thermal equilibrium is studied, has been investigated in great detail and seems to be rather well understood⁽³⁾. Theoretical expectations have been confirmed. It has served, so to speak, as a very reasonable introduction to high temperature plasma physics. This is especially true with respect to the elementary diagnostics. The second one deals mainly with plasmas far from thermal equilibrium and is technologically much more demanding. It has been possible to achieve interesting results on important questions⁽⁴⁾, arising for almost collisionfree plasmas, e.g. on relaxation and dissipation processes. We hope, that we will be able to show, that in this wide field of plasma physics there are many interesting questions left open and are awaiting to be studied.

The plasma initial conditions for this type of experiment and for the second one to be discussed later are summarized in the following table.

Plasma initial conditions

Plasma parameters	Near thermal equilibrium	Far from thermal equilibrium
Density	10^{16} cm^{-3}	10^{13} cm^{-3}
Temperature	2 eV	5 eV
$\beta = 8\pi nkT/B_{ext}^2$	1	1
Compression time t_c	$2 \cdot 10^{-7} \text{ s}$	$4 \cdot 10^{-7} \text{ s}$
Collision time τ_{ii}	$3 \cdot 10^{-10} \text{ s}$	1 μs
Mean free path λ_{ii}	$7 \cdot 10^{-4} \text{ cm}$	5 cm
Sheath width c/ω_{pi}	0.3 cm	10 cm

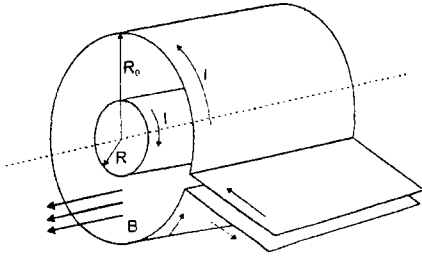
The special case of field-reversed configurations (FRC's) can be dealt with only briefly because of lack of time. The main purpose of this section is to point out the basic aspects of this scheme and turn your attention to it.

GENERAL TECHNICAL AND PHYSICAL FEATURES OF THETA-PINCHES

The principles of a theta-pinch experiment are as follows (Fig. 1). In a straight cylindrical quartz tube is a well conducting, fully ionized gas, e.g. hydrogen, on which a magnetic field B_i eventually is superimposed. The discharge tube is surrounded by a single turn coil, which is connected by way of a switch to a low-inductance capacitor bank. The discharge of the bank generates a magnetic field in the coil and simultaneously causes a current density j in the boundary zone of the plasma. Consequently a magnetic pressure gradient $j \times B$ acts on the plasma (B_{ext} is the axial magnetic field). As soon as the external magnetic pressure becomes greater than the sum of the kinetic pressure of the plasma $n_0 k T_0$ (n_0 = initial particle density of the plasma; T_0 = initial temperature of the plasma) and the pressure of the internal magnetic field $B_i^2/8\pi$, the plasma is accelerated towards the axis of the cylinder.

In general, the experimental arrangement is dimensioned such that the time after which $B_{ext}^2/8\pi \gg n_0 k T_0$, is reached is small compared to the time a_0/v_s (a_0 = initial radius of the plasma; v_s = velocity of a pressure perturbation) which a pressure perturbation needs to move towards the axis. As a consequence a cylindrical hydromagnetic shock wave is generated, which causes an irreversible temperature rise of the plasma behind the shock front. The plasma behind the shock front is acted upon by the magnetic piston, and the plasma cylinder as a whole is thus compressed with supersonic speed. When the shock front arrives at the axis it is reflected and the radial plasma flow is brought to rest. The flow energy is entirely converted into thermal energy. When the reflected shock hits the magnetic piston, the plasma expands until it is in equilibrium with the external magnetic pressure again.

Fig.1 Theta-pinch configuration



We are interested to calculate the plasma conditions of this state from those of the pre-shock, i.e. from the initial state. For this purpose we start from the so-called shock relations. They are identical with those for an ideal gas with a constant ratio of specific heats. For simplicity we consider only the case of strong shocks, i.e. with the Mach-number $M = u_1/c_{S1} \gg 1$. Then we obtain

$$\eta = n_2/n_1 = \frac{(\gamma+1)}{(\gamma-1)} = f+1$$

$$p_2/p_1 = [2\gamma/(\gamma+1)] M^2;$$

$$T_2/T_1 = [(\gamma-1)/(\gamma+1)] p_2/p_1$$

In the laboratory system (shockwave moving with u_1) the following relation holds for the piston velocity

$$m_i u_p^2/2 = (f/2) k T_2;$$

furthermore

$$B_p^2/8\pi = p_2 = n_2 k T_2.$$

If we denote the plasma state behind the reflected shock with the subscript 3, we can write down the equations connecting state 3 and 2; in the strong shock limit:

$$n_3/n_2 = \gamma/(\gamma-1) = (f+2)/2;$$

$$p_3/p_2 = (3\gamma-1)/(\gamma-1) = f+3;$$

$$T_3 = [(f+3)/(f+2)] T_2.$$

The magnetic field pulse for the fast magnetic compression of the plasma will be generated by the sudden discharge of a low-inductance capacitor bank through the compression coil. The discharge is initiated by closing a switch. After a transient phase, after which the radius of the piston a_p will still be of the order a_0 , the voltage at the coil is given by

using
and
one obtains

$$\begin{aligned}
 U_C &= I dL_C/dt ; \\
 U &= 2R_p \pi E_p \\
 L_C &= 1.25 \cdot 10^{-7} \pi (a_0^2 - a_p^2) / l \\
 E_p &= u_p B_p .
 \end{aligned}$$

These equations allow us to derive the following important scaling relations:

$$T_2(K = 1.86 \cdot 10^{10} U_0 (V)/\sqrt{N} (cm^{-1})) \quad \text{and} \quad T_3(K) = 4.5 \cdot 10^{10} U_0 (V)/\sqrt{N} (cm^{-1})$$

The main objectives of the first experiment were:

- generation of a hydrogen plasma of 200 – 300 eV
- collision-dominated, i.e. $\lambda_{ei} \ll a_0$;
- mainly for the study of the shock wave phase of an eventual larger experiment.
- with modest technical expenditure.

These requirements led to the following experimental parameters:

Coil radius	2 cm
Coil length	12 cm
Initial density	$10^{16} cm^{-3}$
U_0	$\approx 20 kV$.

With the stated dimensions the compression coil had an inductance of about 10 nH. This required a very low inductance of $L_B \approx 1$ nH of the capacitor bank, which could only be achieved by switching many capacitors in parallel, together with the accompanying spark gaps as switches⁽⁵⁾. For shock heating the plasma the penetration of the the magnetic field during the build-up phase had to be avoided, i.e., a well conducting nearly fully ionized plasma was needed before shock compression. This was to be prepared by a preheating discharge, which, if possible, should produce no impurities. For this purpose we decided to use an electrodeless ring discharge⁽⁶⁾, which was driven by a small capacitor bank coupled to the compression coil via the collector plate. In order to guarantee an immediate breakdown, a high-frequency transmitter was coupled to the discharge tube, and a discharge was started ahead of the main discharge. By means of an additional capacitor bank, connected to the collector plate, an initial magnetic field of the desired magnitude could be provided. With this procedure it turned out that the generation of highly reproducible well-defined plasmas was possible. Impurity concentrations were below 0.1%.

For the first theta-pinch experiments mainly the following diagnostic methods have been used: Magnetic probes, time-resolved photographic measurements by means of a streak camera, refractivity measurements with the help of microwaves, and plasma spectroscopy. Here we shall refrain from a more detailed discussion.

FAST MAGNETIC COMPRESSION OF A PLASMA NEAR THERMAL EQUILIBRIUM

In Fig. 2 we show a streak photo of plasma compression, taken side-on, and the internal magnetic field on the axis of the coil as function of time, with $N_0 = 1.8 \cdot 10^7 cm^{-1}$ and $B_0 = 900$ G. The radial oscillations of the plasma cylinder after the first maximum compression, as seen in Fig. 2, can be easily understood. During the compression of the plasma cylinder the internal magnetic field increases according to $B_{int}(t) = B_{int}(t=0) \times a^2(t=0)/a^2(t)$. At some point in time equilibrium is reached between the external magnetic pressure and the magnetized plasma. Due to the directed kinetic energy of the particles, the plasma cylinder oscillates beyond this state of equilibrium and is then expanded again by the internal pressure. If attenuation is weak, the oscillations are repeated. From more detailed measurements of $B(r)$ and $n(r)$ at different times we may conclude, that the magnetic flux is conserved during the fast compression and that all plasma particles are captured by the magnetic field. We are

very interested in, what temperature has been reached by the fast plasma compression. This we can learn from Fig. 3:

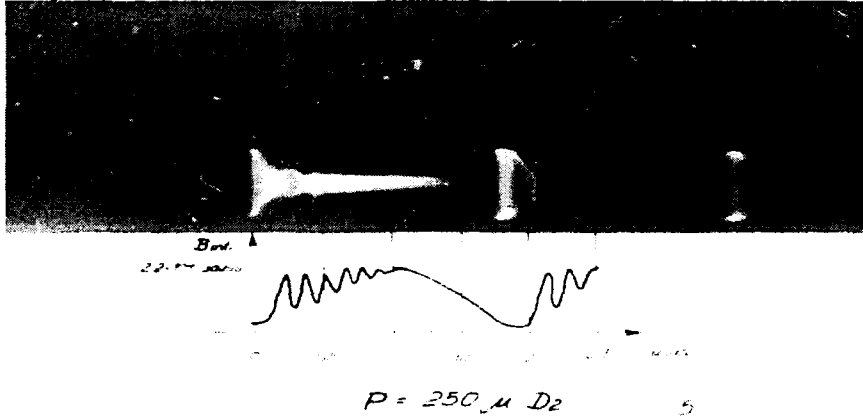
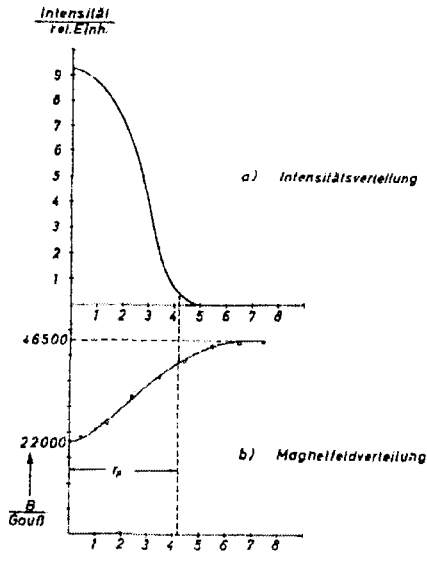


Figure 2. Streak photo of plasma compression and B_{int} as function of time

Figure 3. Radial distribution of magnetic field (b) and of light intensity (a), in relative units



It has been shown, that the impurities in the plasma are negligible⁽⁷⁾. We may assume therefore for the intensity of the radiation emitted by the plasma, that

$$I = n_e^2 T_e^{-1/2}$$

The dependence of the intensity on the temperature is only slight and may be neglected in the interpretation of the intensity distribution as a first approximation.

The line density N is known if we make use of the relation

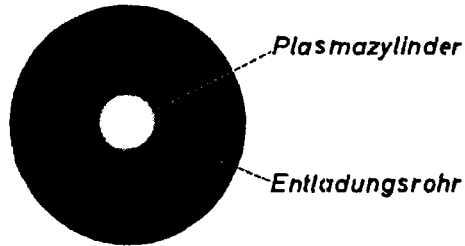
$$\tau = \frac{2\pi}{B_{ext}} (m, N)^{1/2}$$

and determine τ e.g. from Fig. 2. Now the relation

$$N = \int_0^{a_0} n(r) dr$$

can be utilized in order to normalize the distribution and to determine the maximum density $n_{max} = 4.7 \times 10^{17} \text{ cm}^{-3}$.

The measurement of radial distributions is persistent only, if rotational symmetry exists. In order to test this assumption, the plasma was photographed under axial observation at an exposure time of 1×10^{-7} s at the instant of maximum compression. A Kerr cell was used as fast shutter. Figure 4 shows such a photograph.



Belichtungszeit - 10^{-7} sec

Figure 4: Photograph of the plasma cylinder at maximum compression

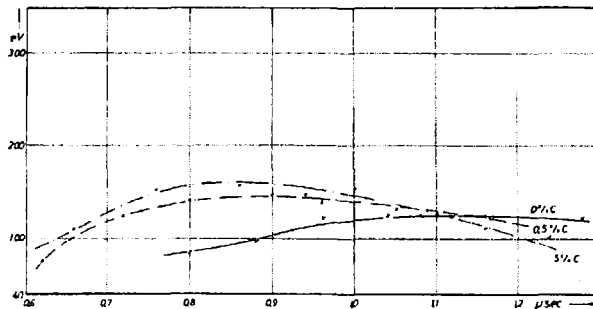
The deviations from rotational symmetry of the plasma cylinder are very minor. The axes of discharge tube and of plasma cylinder coincide.

From the magnetic field distribution we derive $\beta_{\max} = 0.8$ in the vicinity of the axis; for the particle density on the axis we obtained $n_{\max} = 4,5 \cdot 10^{17} \text{ cm}^{-3}$. Now we can calculate the mean energy:

$$k(T_e + T_i) = 1.2 \cdot 10^2 \text{ eV.}$$

From the equation utilized for the calculation of the dimensions follows $k(T_e + T_i) = 1.3 \cdot 10^2 \text{ eV}$.

One may assume, that initially the energy will be predominantly with the ions. To investigate this question we have measured the electron temperature independently. T_e was determined from the ratio of soft x-ray intensities transmitted through Be and Al foils assuming a Maxwellian distribution of electron velocities. T_e as a function of time measured side-on by this foil method is shown in Fig. 5.



At 0% carbon impurity the plasma reaches $T_e = 100 \text{ eV}$ after about $0.8 \mu\text{s}$, the lowest T_e measurable with the existing method. Then it rises rapidly even after peak magnetic field. T_e shows an unexpected increase near the peak magnetic field. This may be caused by end effects, energy transfer from ions to electrons or by magnetic field diffusion.

Figure 5. $T_e(t)$ for increasing concentrations of carbon in $250 \mu \text{ D}_2$

STUDIES OF A HIGH- β , LOW-DENSITY PLASMA FAR FROM THERMAL EQUILIBRIUM

Our experience with straight theta-pinchs gave rise to the hope that the fast magnetic compression of a highly ionized afterglow plasma might be one way to produce a plasma with thermonuclear temperatures. From the scaling law of plasma heating by fast magnetic compression we inferred that we had to work at high voltage and low density. On the basis of existing low-inductance commercial capacitors and by using a new technique of voltage doubling we planned to provide a voltage of 120 kV at the compression coil. From detailed studies of plasma preheating we learned that it would be possible to generate an almost fully ionized hydrogen plasma at a density of $5 \times 10^{12} \text{ cm}^{-3}$ for fast compression. These were the design parameters of the low-density high-voltage theta-pinch at the IPP. Main objectives were:

- Thermonuclear temperature,
- Volume compression ratio of about 10
- Study of relaxation phenomena
- Investigation of the current sheath.

The electrical circuit of the 120 kV experiment is shown in Fig. 6

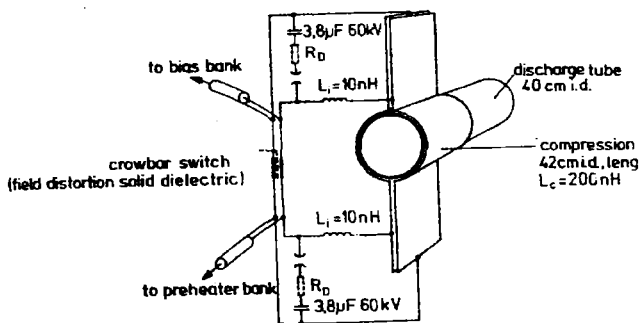


Figure 6. 120 kV theta-pinch experiment (4)

In addition to the diagnostic methods already described, Thomson scattering of laser light was applied for the determination of electron density and electron temperature. Electric fields in the plasma, interpreted as turbulent fields, have been determined by the ratio of forbidden to allowed line intensity of two neutral He lines ($\lambda = 4472 \text{ \AA}$; $\lambda = 4922 \text{ \AA}$;) using the equation given by Baranger and Mozer⁽⁸⁾. Mean ion energies were determined by measuring the neutron yields and, in addition, by using the pressure balance equation. Results are shown in Fig. 7.

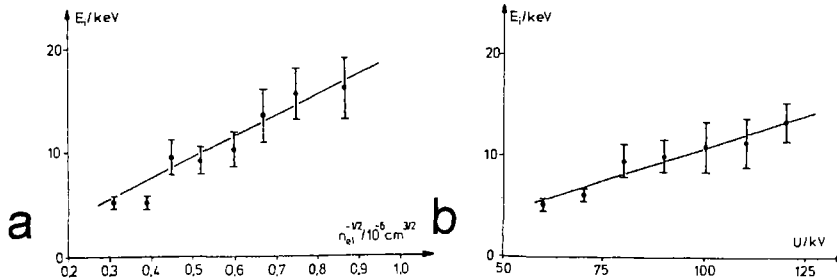


Figure 7. Mean ion energy as a function of initial density (a), and as function of voltage (b)

In order to determine the development of the radial plasma flow, the time history of the electron density pulse generated by the piston has been measured. Figure 8 shows an example at $a_p = 8$ cm. The velocity of the first two peaks is about twice the piston velocity. The third peak coincides with the piston and its velocity is about equal to that of the sheath, as measured by magnetic probes. Most of the initial plasma is trapped by the piston. We may conclude, that the first two density pulses are generated by the magnetic piston at the beginning of the implosion by elastic reflection of particles. After a short time the reflection properties of the piston change, probably because of the development of micro-instabilities in the current sheath. As a result of the turbulence, the plasma encountered by the piston is trapped and electrons as well as ions are heated.

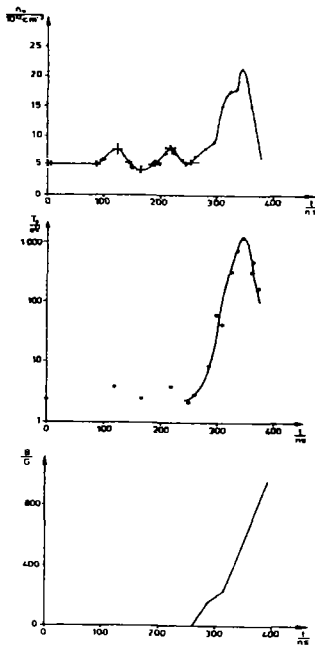


Figure 8. $n_e(t)$, $T_e(t)$ and $B(t)$ for $a_p = 8$ cm

When the magnetic piston passes $R=8$ cm, 80% of the total kinetic energy of the particles is stored in the flow energy of the ions. Upon reflection at the axis most of the ion flow energy is converted into random energy perpendicular to the magnetic field. At 800 ns the ion velocity distribution has almost approached a Gaussian. The mean ion energy derived from end-on measurements is smaller by a factor of 4. T_e near the axis approaches 30eV and is determined by the balance between energy transfer from the ions and heat conduction losses to the ends.

REMARKS ON FIELD-REVERSED CONFIGURATIONS (FRC's)

We have also done some investigation on low- β plasmas. Here we shall deal only with one special case, when an initial magnetic field of -2500 G is superimposed on the preheated plasma. The minus sign here means that the direction of the initial magnetic field is antiparallel to the compression field.

Let us consider the conditions immediately after the compression field is switched on. The magnetic field between plasma boundary and the wall will, for a short time, become zero. As a consequence the pressure of the internal magnetic field will drive the plasma towards the wall. Then the pressure of the reversed field will be built up again. It soon will exceed that of the internal field and then compression starts again. At some point we may stop the further increase of B_{ext} . The most interesting development will happen at the ends of the compression coil. The magnetic field lines close and a configuration with closed magnetic field lines, i.e. a toroidal system, will develop (Fig. 9).

Densities and temperatures achieved in theta-pinchs with trapped reverse field seem to be similar to those in standard theta-pinchs. Impurity concentrations are somewhat higher. Concerning the main loss mechanism in theta-pinchs, our experience was. that the comparatively high concentration of

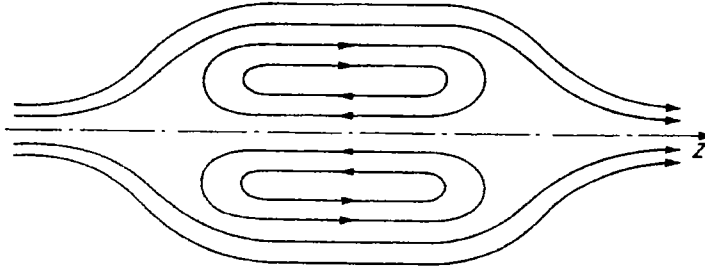


Figure 9. Field-reversed configuration of a theta-pinch

neutral hydrogen (e.g. 50%) leads to correspondingly high losses due to charge exchange. This should also be the case for FRC's. We have found no way to avoid these losses.

However, there have been successful attempts to transfer FRC's into different vacuum chambers⁽⁹⁾. This way it might be possible to get rid of the neutral particle background. The possibility to transfer large numbers of hot ions by means of FRC's (e.g. into tokamaks) could raise new interest in research on this type of theta-pinchs.

REFERENCES

- (1) "Plasma Physics and Controlled Nuclear Fusion"; 1962, Supplement Part 2, IAEA Vienna. (1962).
- (2) P. Bogen and E. Hintz; "Shock Induced Plasmas" in "Gaseous Electronics", M.N. Hirsch and H.J. Oskam, eds., Academic Press (1978).
- (3) E. Hintz; Plasma Physics and Contr. Nucl. Fusion Res., Suppl. Part 2, IAEA Vienna; 601 (1962).
- (4) P. Bogen, et al.; Plasma Phys. Contr. Nucl. Fusion Res.; 3, 349 (1975).
- (5) H. Beerwald and E. Hintz; 1960, Proc. 4 th Int. Conf. Ion. Phen. Gases, Uppsala, North-Holland Publ., Amsterdam; 2, 468 (1960).
- (6) H. Beerwald, P. Bogen, T. El-Khalafawi, H. Fay, E. Hintz, and H. Kever; Nucl. Fusion Suppl., IAEA Vienna; Part 2, 595 (1962).
- (7) P. Bogen, E. Hintz, J. Schlüter; Phys. Fluids; 7, (1964).
- (8) M. Baranger, B. Mozer; Phys. Rev.; 123, 25 (1961).
- (9) A.G. Es'kov, et al.; Plasma Phys. and Contr. Nucl. Fusion 1976, IAEA Vienna; 2, 187 (1976).